Electronic Supporting Information

Pt nanoparticles anchored over Te nanorods as a novel and promising catalyst for methanol oxidation reaction

Xudong Yang, Jia Xue and Ligang Feng*

School of Chemistry and Chemical Engineering Yangzhou University, Yangzhou, 225002, PR China.

Email: ligang.feng@yzu.edu.cn; fenglg11@gmail.com (L Feng*)

Experimental methods

Chemicals and materials

All the reagents in the experiment were analytical grade and used as received. Sodium tellurate ($NaTeO_3$), hexachloroplatinic acid ($H_2PtCl_6 \cdot 6H_2O$), ethylene glycol ($C_2H_6O_2$), polyvinylpyrrolidone (Mw=58000) (PVP) and L-ascorbic acid were purchased from Shanghai Aladdin Bio-Chem Technology Co., Ltd. Potassium hydroxide (KOH) and sulphuric acid (H_2SO_4) were purchased from Sinopharm Chemical Reagent Co., Ltd. Nafion (5 wt.%) was purchased from Sigma-Aldrich. All solutions were prepared with ultrapure water (Thermo Fisher Scientific (USA) Co., Ltd). Commercial Pt/C and PtRu/C catalysts were purchased from Johnson Matthey Chemicals Ltd for reference. The commercial Pt/C catalyst with 20 wt.% Pt loading was purchased with the average particle size of about 3.5 nm.[1-3] The commercial PtRu/C catalyst with 20 wt.% Pt and 10 wt.% Ru loading and 70 wt.% carbon was purchased with the average particle size of about 3.3 nm.[4]

Preparation of Pt/Te nanorods

The synthesis of Pt/Te nanorods consisted of two steps:

(1) Preparation of Te nanorods

In the first step, 230 mg $NaTeO_3$, 450 mg L-ascorbic acid, and 100 mg PVP were added into a beaker and dispersed in 30 mL of ethylene glycol under vigorous magnetic stirring at room temperature to form a homogeneous solution. The obtained solution was transferred into the Teflon-lined stainless steel with a volume capacity of 50 mL, sealed and reacted at 150^{o}C for 6 h. Finally, the Te nanorods were precipitated using acetone, cleaned with ultrapure water and dried overnight in vacuum at 60^{o}C.

(2) Preparation of Pt/Te nanorods

In the second step, the platinum nanoparticles anchored over Te nanorods were prepared by rapid microwave-assisted ethylene glycol reduction process. Briefly, 0.025 g Te nanorods obtained above were ultrasonically dispersed in 100 mL ethylene glycol to form a uniform suspension. Under stirring, a certain amount of H_2PtCl_6 solution (contain 10 mg Pt) was added to the suspension. The suspension was placed and exposed in the middle of a microwave oven with 700 W with 60

s and cooled to room temperature naturally. At last, the suspension was filtered, washed and dried overnight at 60°C in a vacuum oven to obtain Pt/Te nanorods catalyst. The main advantages of microwave irradiation include a very short thermal induction period and the generation of localized high temperatures at the reaction sites resulting in a fast rate of metal reduction. The reaction mechanism for Pt nanoparticles fabrication was proposed as below using the ethylene glycol:

$$CH_2OH\text{-}CH_2OH = CH_3CHO + H_2O \quad (1)$$

$$2CH_3CHO + PtCl_6^{2-} + 6OH^- = Pt + 6Cl^- + 2CH_3COO^- + 4\ H_2O \quad (2)$$

Physical characterizations

The catalysts are characterized on Bruker D8 advance X-ray diffraction (XRD) with Cu Kα radiation. X-ray photoelectron spectroscopy (XPS) measurement are carried on an ECSALAB250Xi S3 spectrometer with an Al Kα radiation source. The morphology is examined with a FEI Sirion-200 scanning electron microscope (SEM) and a transmission electron microscope (TEM) operating at 200 kV. X-ray detector spectrum (EDS) images are obtained on a TECNAI G2 F30 transmission electron microscope (acceleration voltage: 300 kV). The accurate element content was determined by the Optima 7300 DV inductively coupled plasma optical emission spectroscopy (ICP-AES).

Electrochemical Pre-treatment

All the electrochemical measurements are carried out with a Bio-Logic VSP electrochemical workstation (Bio-Logic Co., France) and a conventional three-electrode system. The working electrode is a glassy carbon electrode (3 mm diameter, 0.07 cm^{-2}). The graphite rod and the saturated calomel electrode (SCE, Hg/Hg_2Cl_2) serve as a counter and a reference electrode through a double salt-bridge and luggin capillary tip, the potential was carefully checked before and after the relevant measurements. The catalyst ink was prepared by ultrasonically dispersing a mixture containing 2 mg of catalyst and 0.5 mg carbon black, 475 μL of ethanol and 25 μL of a 5 wt. % Nafion solution. Next, 10 μL of the catalyst ink was pipetted onto a pre-cleaned working electrode.

Cyclic Voltammetry Measurements

The activities of catalysts for methanol electro-oxidation were measured. The measurements in acid electrolyte were carried out at room temperature in 0.5 M H_2SO_4+1 M CH_3OH solution at a potential range between -0.2 and 1.0 V vs. SCE

and at a potential scan rate of 50 mV s^{-1}. The measurements in alkaline solution were carried out at room temperature in 1 M KOH+ 1 M CH_3OH solution at a potential range between -1 and 0.2 V vs. SCE and at a potential scan rate of 50 mV s^{-1}.

CO stripping measurements

For acidic methanol oxidation, 99.99% CO was subsequently bubbled in the 0.5 M H_2SO_4 for 15 min when the potential was controlled to be 0 V vs. SCE. The excess CO in the electrolyte was purged out with N_2 for 15 min. The CO stripping was performed in the potential of the range -0.2 ~ 1.0 V vs. SCE at a scan rate of 20 mV s^{-1}. Similarly, for alkaline methanol oxidation, the potential was controlled to be -0.8 V vs. SCE and the CO stripping was performed in the potential of the range -1 ~ 0.2 V vs. SCE at a scan rate of 20 mV s^{-1}. The electrochemical active surface areas (ECSA) and the tolerance to CO poisoning were estimated by the CO stripping test, assuming that the coulombic charge required for the oxidation of the CO monolayer was 420 μC cm^{-2}.

Chronoamperometry measurements

To estimate the stability of the catalysts for acidic methanol oxidation, the chronoamperometry (CA) experiments were performed in 0.5 M H_2SO_4 and 1 M CH_3OH solution at 0.55 V vs. SCE; for alkaline methanol oxidation, the CA experiments were performed in 1 M KOH and 1 M CH_3OH solution at -0.26 V vs. SCE.

Electrochemical Impedance Measurements

The electrochemical impedance spectra (EIS) were recorded at the frequency range from 1000 kHz to 30 mHz with 12 points per decade. The amplitude of the sinusoidal potential signal was 5 mV.

Supporting Tables and Figures

Table S1. Binding energies of the Pt $4f_{7/2}$ and Pt $4f_{5/2}$ components for the Pt/Te nanorods and Pt/C catalyst.

Catalysts	Pt $4f_{7/2}$		Pt $4f_{5/2}$		Relative content of
	Peak	Bind energy/ eV	Peak	Bind energy/ eV	Pt^0/ %
Pt/Te nanorods	Pt^0	71.3	Pt^0	74.6	93.5%
	Pt^{2+}	72.3	Pt^{2+}	75.3	
Pt/C	Pt^0	71.6	Pt^0	74.9	80.2%
	Pt^{2+}	72.6	Pt^{2+}	76.6	

Table S2. Binding energies of the Te $3d_{5/2}$ and Te $3d_{3/2}$ components for the Pt/Te nanorods and Te nanorods.

Catalysts	Te $3d_{5/2}$		Te $3d_{3/2}$		Relative content of Te^{4+}/
	Peak	Bind energy/ eV	Peak	Bind energy/ eV	%
Pt/Te nanorods	Te^0	572.9	Te^0	583.3	78.5%
	Te^{4+}	576.1	Te^{4+}	586.5	
Te nanorods	Te^0	572.8	Te^0	583.2	68.1%
	Te^{4+}	576.1	Te^{4+}	586.5	

Table S3. Electrochemical active surface area (ECSA) estimation from CO stripping voltammetry experiment and peak potential for CO stripping for Pt/Te nanorods, Pt/C, and PtRu/C catalysts in 0.5 M H_2SO_4 with a scan rate of 20 mV s^{-1}.

Catalysts	ECSA/ m^2 g_{Pt}^{-1}	Peak Potential/ V vs.SCE
Pt/Te nanorods	84.6	0.52
Pt/C	65.3	0.57
PtRu/C	80.5	0.51

Table S4. Mass activity and specific activity expressed as the positive peak current density of Pt/Te nanorods, Pt/C and PtRu/C catalysts in 0.5 M H_2SO_4+1 M CH_3OH solution.

Catalysts	Mass activity/ mA mg_{Pt}^{-1}	Specific activity/ mA cm^{-2}
Pt NPs/Te NRs	762	0.90
Pt/C	268	0.41
PtRu/C	346	0.42

Table S5. Comparisons of activities of various electrocatalysts for methanol oxidation in acidic media. The scan rate was 50 mV s^{-1}.

Catalysts	Mass activity /mA mg_{Pt}^{-1}	Condition	Reference
Pt/Te nanorods	762	0.5 M H_2SO_4+1 M CH_3OH	This work
Commercial Pt/C-JM	280	0.5 M H_2SO_4+1 M CH_3OH	[3]
Commercial PtRu/C-JM	348	0.5 M H_2SO_4+1M CH_3OH	[4]
Pt_1Ru_3 nanosponges	410	0.5 M H_2SO_4+1 M CH_3OH	[5]
PtPdTe nanowires	595	0.5 M H_2SO_4+1 M CH_3OH	[6]
TePbPt nanotubes	532	0.5 M H_2SO_4+1 M CH_3OH	[7]
Au@Pd@Pt nanoparticles	430	0.5 M H_2SO_4+1 M CH_3OH	[8]
Ultrathin Pt nanowires	581	0.5 M H_2SO_4+1 M CH_3OH	[9]
PtIrTe nanotubes	495	0.5 M H_2SO_4+1 M CH_3OH	[10]
Pt Nanoparticles	460	0.5 M H_2SO_4+1 M CH_3OH	[11]
Pt–Pd Hollow Nanoparticles	580	0.5 M H_2SO_4+1 M CH_3OH	[12]
Pt–WC/graphene	687	1 M H_2SO_4+1 M CH_3OH	[13]

Table S6. EIS fitting parameters from equivalent circuits for different catalysts in the 0.5 M H_2SO_4 +1 M CH_3OH solution.

Catalysts	L/ H	R_s/ Ω	R_{CT}/ Ω	R_o/ Ω	CPE/S s^{-n}
Pt/Te nanorods	5.2E-25	6.5	1100	31.6	6.1E-5
Pt/C	3.9E-24	6.7	1900	40.5	4.5E-4
PtRu/C	2.2E-25	6.6	1450	38.5	5.2E-4

Table S7. Electrochemical active surface area (ECSA) estimation from CO stripping experiment and peak potential for CO stripping for Pt/Te nanorods, Pt/C and PtRu/C catalysts in 1 M KOH solution with a scan rate of 20 mV s^{-1}.

Catalysts	ECSA/ m^2 g_{Pt}^{-1}	Peak Potential/ V vs.SCE
Pt/Te nanorods	73.1	-0.42
Pt/C	58.8	-0.45
PtRu/C	70.6	-0.39

Table S8. Mass activity and specific activity expressed as the positive peak current density of Pt/Te nanorods, Pt/C and PtRu/C catalysts in 1 M KOH +1 M CH_3OH solution.

Catalysts	Mass activity/ mA mg_{Pt}^{-1}	Specific activity/ mA cm^{-2}
Pt/Te nanorods	823	1.13
Pt/C	297	0.51
PtRu/C	370	0.52

Table S9. Comparisons of activities of various electrocatalysts for methanol oxidation in alkaline media. The scan rate was 50 mV s^{-1}.

Catalysts	Mass activity /mA mg_{Pt}^{-1}	Condition	Reference
Pt NPs/Te NRs	823	1 M KOH+1 M CH_3OH	This work
Pt/C	297	1 M KOH+1 M CH_3OH	This work
PtRu/C	371	1 M KOH+1 M CH_3OH	This work
Pt/rGO	400	1 M KOH+1 M CH_3OH	[14]
Cu–Pt coral-like nanoparticles	263	1 M KOH+1 M CH_3OH	[15]
RuTe/PdAu NTs	540	1 M KOH+1 M CH_3OH	[16]
Commercial Pt blacks	610	1 M KOH+1 M CH_3OH	[17]
Fe_3O_4@CeO_2/Pt	273	1 M KOH+1 M CH_3OH	[18]
Pt/C (TKK)	690	1 M KOH+1 M CH_3OH	[19]

Table S10. EIS fitting parameters from equivalent circuits for different catalysts in the 1 M KOH +1 M CH_3OH solution.

Catalysts	L_1/ H	R_S/ Ω	R_{CT}/ Ω	R_0/ Ω	CPE_1/S s^{-n}
Pt NPs/Te NRs	7.0E-6	8.1	38.8	4.8	4.2E-5
Pt/C	8.2E-5	8.3	126.4	6.4	6.2E-4
PtRu/C	6.4E-5	8.2	72.6	5.9	7.6E-4

Table S11. The composition of Pt and Te determined by ICP for Pt/Te nanorods

Catalysts	Pt/ at.%	Te/ at.%
Pt/Te nanorods	18.1%	81.9%
After 24 h CA test in 0.5 M H_2SO_4+1 M CH_3OH	19.2%	80.8%
After 24 h CA test in 1 M KOH+1 M CH_3OH	19.6%	80.4%

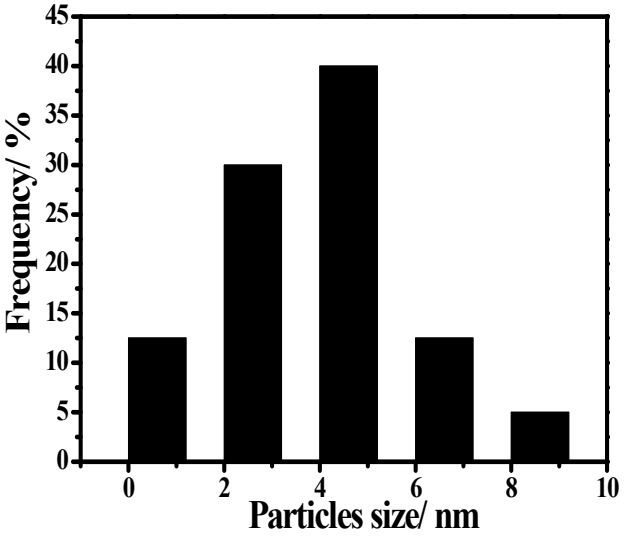

Figure S1. The particle size distribution histogram of Pt/Te nanorods.

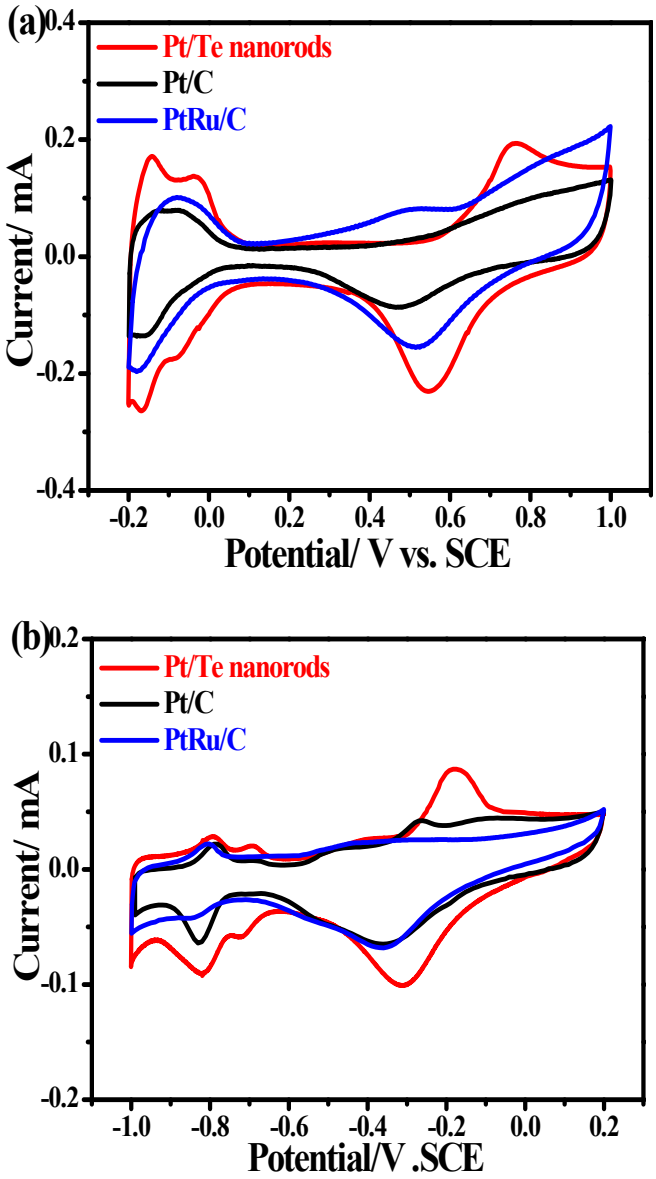

Figure. S2 Cyclic voltammograms of Pt/Te nanorods, Pt/C and PtRu/C catalysts recorded in N_2-saturated 0.5 M H_2SO_4 solution (a) and 1 M KOH solution (b), respectively.

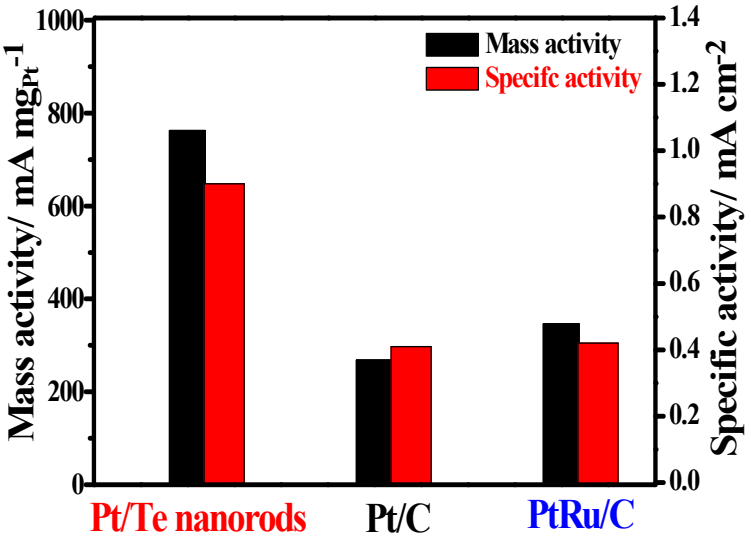

Figure S3. Graphical comparison of mass and specific activity of Pt/Te nanorods, Pt/C and PtRu/C catalysts recorded in N_2-saturated 0.5 M H_2SO_4 + 1 M CH_3OH solution at a scan rate of 50 mV s^{-1}.

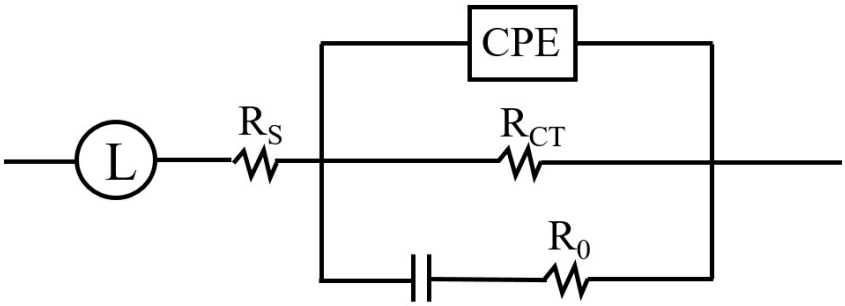

Figure S4. The equivalent circuit for the EIS data fitting in the acid electrolyte. For the equivalent circuit, the R_S represents the uncompensated solution resistance; R_{CT} corresponds to the charge-transfer resistance arising from alcohols oxidation; R_0 is probably related to the contact resistance between the catalyst material and the glassy carbon electrode; the constant phase element (CPE) composition is for double-layer capacitance; and the L usually comes from the external circuit inductance and usually does not involve an electrochemical process.

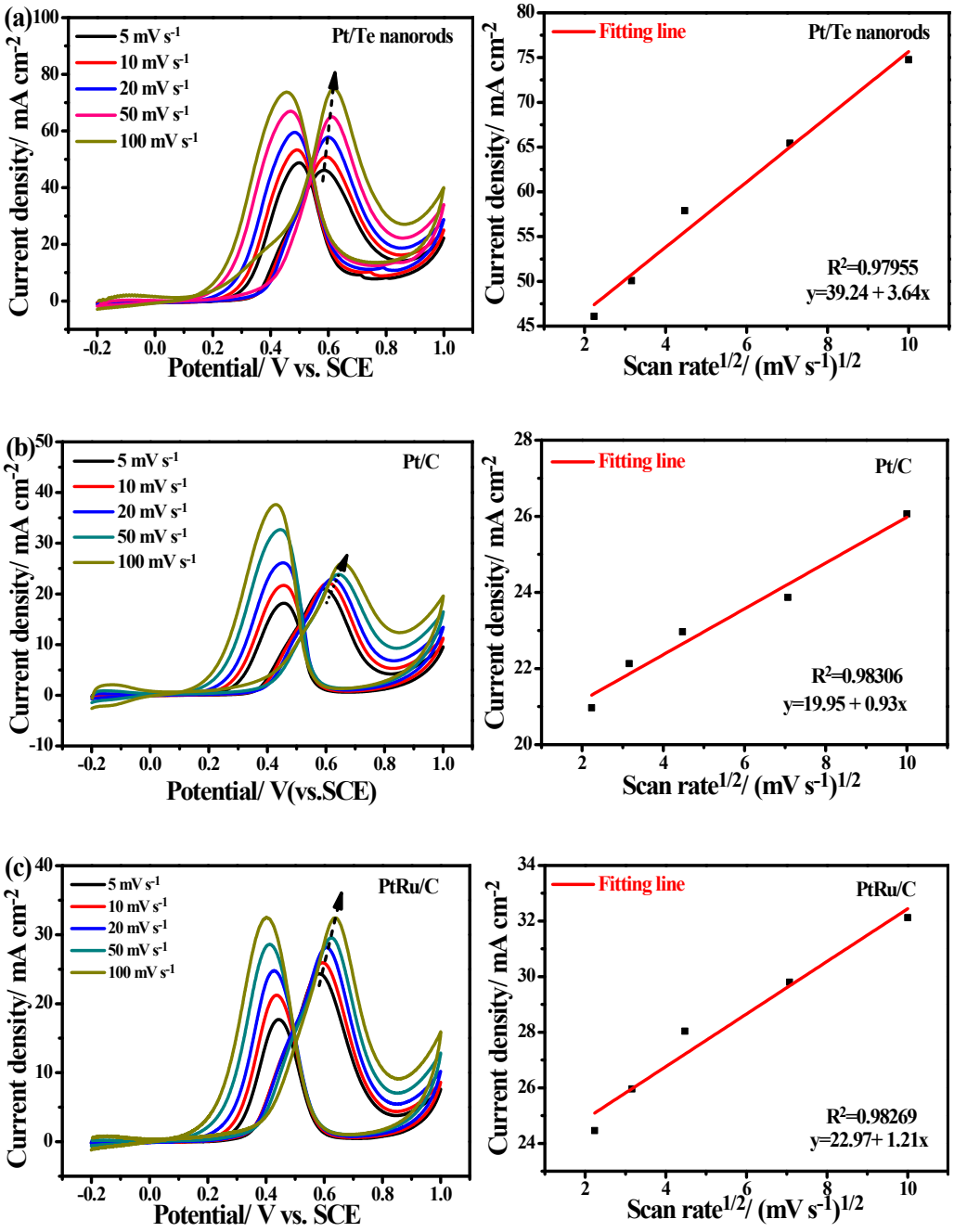

Figure S5. Cyclic voltammograms of the Pt/Te nanorods (a), Pt/C (b) and PtRu/C (c) catalysts in 0.5 M H_2SO_4+1 M CH_3OH at scan rates of 5, 10, 20, 50, 100 mV s^{-1} and the corresponding peak current density versus the square root of the scan rates.

The linear relationship was attributed to a diffusion-controlled process. The relationship between the peak current density and the square root of scan rates complies with the following equation[20]: $i_p=2.99\times10^5n(\alpha n')^{1/2}AC_\infty D_0^{1/2}v^{1/2}$, where Where i_p is the peak current density, n is the electron-number for the total reaction, n′ is the electron- number transferred in the rate-determining step, α is the electron transfer coefficient of the rate-determining step, A is the electrode surface

area, C_∞ is the bulk concentration of the reactant, D_0 is the diffusion coefficient, v is the potential scan rate. In this paper, the slope of the i_p vs. the square scan rate. In the same electrolyte and the same reaction, the parameters n, C_∞ and D_0 are constant; therefore, the slope is decided by $\alpha n'$. It can be said that the synergy effect between Pt and Te greatly increases the electron transfer rate in the electrolysis process and lead to the excellent electrochemical activity for methanol electrooxidation.

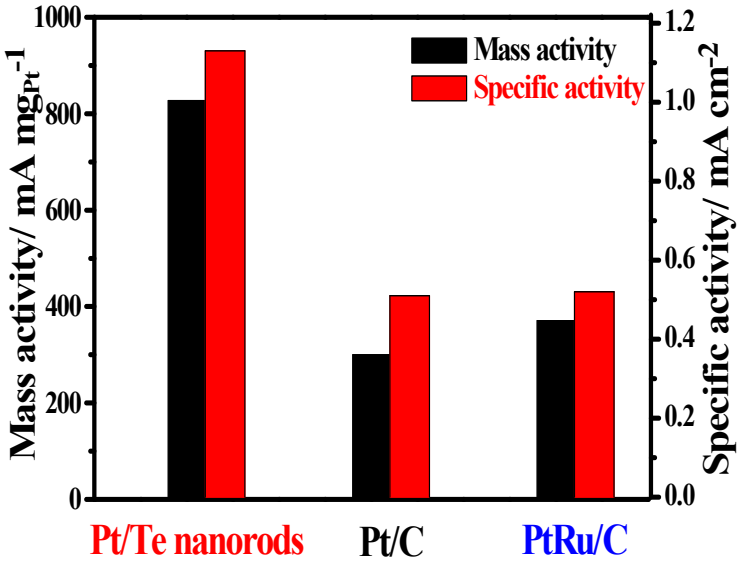

Figure S6. Graphical comparison of mass and specific activity of Pt/Te nanorods, Pt/C and PtRu/C catalysts recorded in N_2-saturated 1 M KOH + 1 M CH_3OH solution at a scan rate of 50 mV s^{-1}.

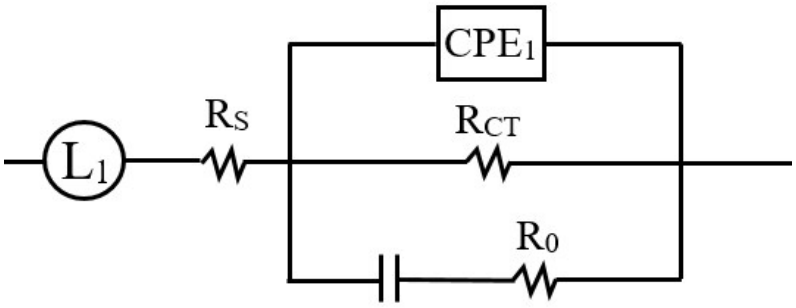

Figure S7. The equivalent circuit for the EIS fitting in the alkaline electrolyte. For the equivalent circuit, the R_S represents the uncompensated solution resistance; R_{CT} corresponds to the charge-transfer resistance arising from alcohols oxidation; R_0 is probably related to the contact resistance between the catalyst material and the glassy carbon electrode; the constant phase element (CPE_1) composition is for double-layer capacitance; and the L_1 usually comes from the external circuit inductance and usually does not involve an electrochemical process.

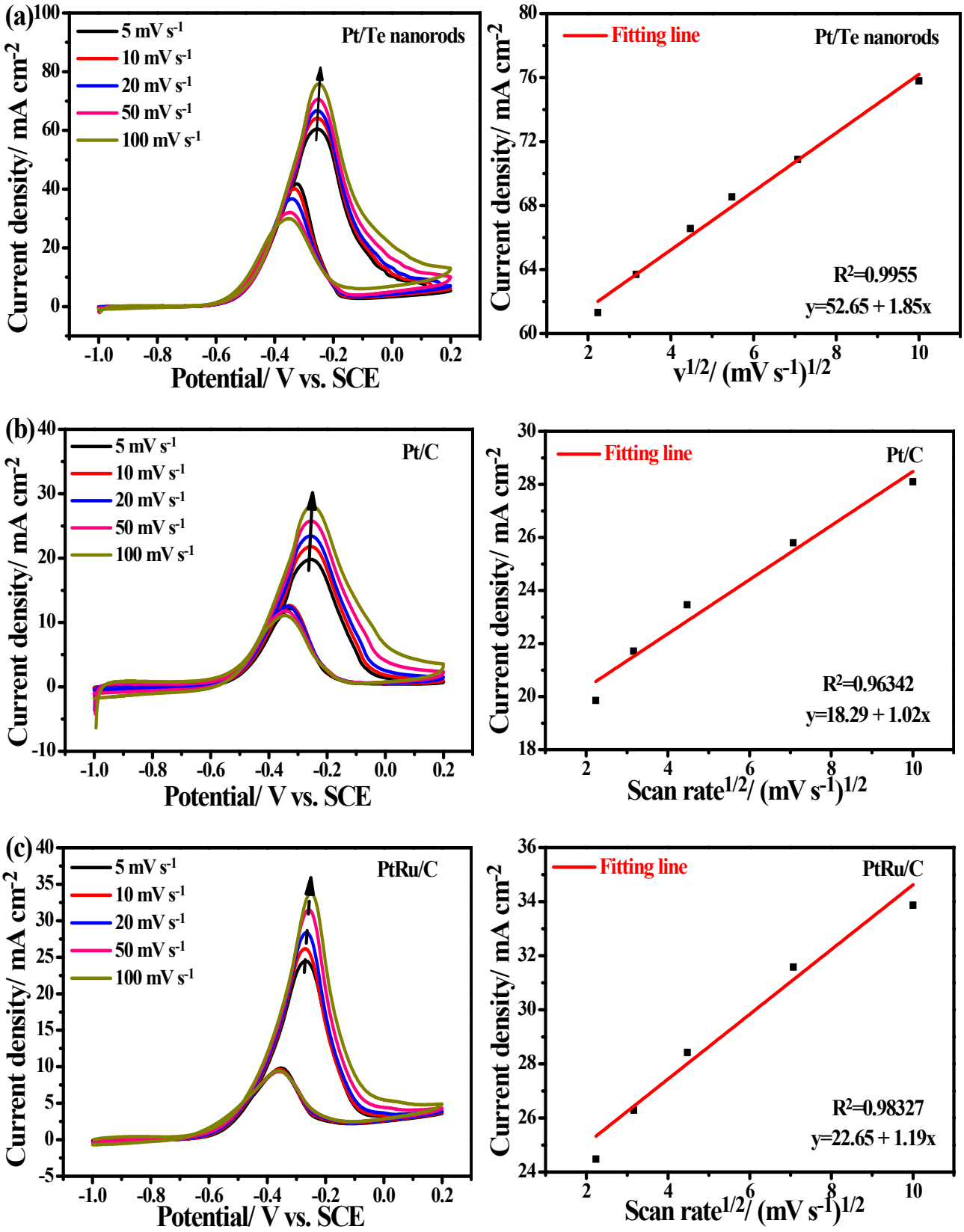

Figure S8. Cyclic voltammograms of the Pt/Te nanorods (a), Pt/C (b) and PtRu/C (c) catalysts in 1 M KOH+1 M CH_3OH solution at scan rates of 5, 10, 20, 50, 100 mV s^{-1} and the corresponding peak current density versus the square root of the scan rates.

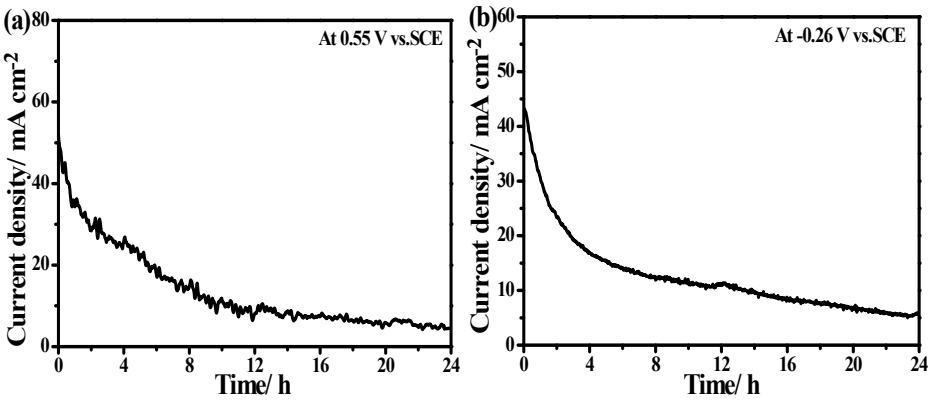

Figure S9. Chronoamperometry curves of Pt/Te nanorods recorded for 24 h at 0.55 V in N_2 saturated 0.5 M H_2SO_4 + 1 M CH_3OH solution (a) and at -0.26 V in N_2 saturated 1 M KOH + 1 M CH_3OH solution (b), respectively. The current decay was consistent with the trend of Cottrell equations.

References

1. J. Chang, L. Feng, K. Jiang, H. Xue, W.-B. Cai, C. Liu and W. Xing, *J. Mater. Chem. A*, 2016, **4**, 18607-18613.
2. S. Yao, L. Feng, X. Zhao, C. Liu and W. Xing, *J. Power Sources*, 2012, **217**, 280-286.
3. J. Chang, L. Feng, C. Liu, W. Xing and X. Hu, *Energy Environ. Sci.*, 2014, **7**, 1628.
4. L. Feng, K. Li, J. Chang, C. Liu and W. Xing, *Nano Energy*, 2015, **15**, 462-469.
5. M. Xiao, L. Feng, J. Zhu, C. Liu and W. Xing, *Nanoscale*, 2015, **7**, 9467-9471.
6. L. Hui-Hui, Z. Shuo, G. Ming, C. Chun-Hua, H. Da, L. Hai-Wei, W. Liang and Y. Shu-Hong, *Angew. Chem., Int. Ed.*, 2013, **52**, 7472-7476.
7. L. Yang, G. Li, J. Ge, C. Liu, Z. Jin, G. Wang and W. Xing, *J. Mater. Chem. A*, 2018, **6**, 16798-16803.
8. L. Wang and Y. Yamauchi, *Chem. Mater.*, 2011, **23**, 2457-2465.
9. L. Ruan, E. Zhu, Y. Chen, Z. Lin, X. Huang, X. Duan and Y. Huang, *Angew. Chem., Int. Ed.*, 2013, **52**, 12577-12581.
10. Y. Hao, Y. Yang, L. Hong, J. Yuan, L. Niu and Y. Gui, *ACS Appl. Mater. Interfaces*, 2014, **6**, 21986-21994.
11. H. Meng, F. Xie, J. Chen, S. Sun and P. K. Shen, *Nanoscale*, 2011, **3**, 5041-5048.
12. L. Wang and Y. Yamauchi, *J. Am. Chem. Soc*, 2013, **135**, 16762-16765.
13. R. Wang, Y. Xie, K. Shi, J. Wang, C. Tian, P. Shen and H. Fu, *Chem. - Eur. J.*, 2012, **18**, 7443-7451.
14. D. Liu, L. Yang, J. S. Huang, Q. H. Guo and T. Y. You, *RSC Adv.*, 2014, **4**, 13733-13737.
15. S. Kang, G. Gao, X. Xie, T. Shibayama, Y. Lei, Y. Wang and L. Cai, *Mater. Res. Lett.*, 2016, **4**, 212-218.
16. W. Hong, J. Wang and E. Wang, *J. Mater. Chem. A*, 2015, **3**, 13642-13647.
17. W. Hong, J. Wang and E. Wang, *Nano Res.*, 2015, **8**, 2308-2316.

18. Q. Wang, Y. Li, B. Liu, Q. Dong, G. Xu, L. Zhang and J. Zhang, *J. Mater. Chem. A*, 2015, **3**, 139-147.
19. Z. Yin, M. Chi, Q. Zhu, D. Ma, J. Sun and X. Bao, *J. Mater. Chem. A*, 2013, **1**, 9157-9163.
20. Y. Wang, B. Wu, Y. Gao, Y. Tang, T. Lu, W. Xing and C. Liu, *J. Power Sources*, 2009, **192**, 372-375.